Quantum Phase Transition in the Sub-Ohmic Spin-Boson Model: Quantum Monte Carlo Study with a Continuous Imaginary Time Cluster Algorithm

André Winter,[1] Heiko Rieger,[1] Matthias Vojta,[2] and Ralf Bulla[2]

[1]*Theoretische Physik, Universität des Saarlandes, 66041 Saarbrücken, Germany*
[2]*Institut für Theoretische Physik, Universität zu Köln, Zülpicher Straße 77, 50937 Köln, Germany*
(Received 29 July 2008; published 20 January 2009)

A continuous time cluster algorithm for two-level systems coupled to a dissipative bosonic bath is presented and applied to the sub-Ohmic spin-boson model. When the power s of the spectral function $J(\omega) \propto \omega^s$ is smaller than 1/2, the critical exponents are found to be classical, mean-field like. Potential sources for the discrepancy with recent renormalization group predictions are traced back to the effect of a dangerously irrelevant variable.

Quantum-mechanical systems embedded into a dissipative environment play an important role in many areas of physics [1,2]. Among the numerous applications of models that couple a small quantum system to a bosonic bath are noisy quantum dots [3], decoherence of qubits in quantum computations [4], and charge transfer in donor-acceptor systems [5]. A major research field is quantum impurity models (i.e., a quantum spin embedded in a crystal [6]), where, in particular, quantum critical points occurring for instance in the Bose-Fermi Kondo model have been studied intensively [7–10].

The paradigmatic model of a two-state system coupled to an infinite number of bosonic degrees of freedom, characterized by its spectral function $J(\omega)$ with low-frequency behavior $J(\omega) \propto \omega^s$, is the spin-boson (SB) model [1,2]. As a function of the strength of the coupling to its bath, it displays for $s \leq 1$ a quantum phase transition (QPT) at zero temperature between a delocalized phase, which allows quantum-mechanical tunneling between the two states, and a localized phase, in which the system behaves essentially classically.

While the phase transition is understood in the case of Ohmic dissipation ($s = 1$), the sub-Ohmic situation ($s < 1$) has been investigated in detail only recently. On general grounds, one expects the phase transition to fall into the same universality class as that of the classical Ising spin chain with long-range interactions [11]. Indeed, a continuous QPT has been found in the spin-boson model for all values of $0 < s < 1$ [12], using a generalization of Wilson's numerical renormalization group (NRG) technique [6]. However, on the basis of these NRG calculations, it was suggested that the quantum-to-classical mapping fails for $s < 1/2$ [13]: There, the Ising chain displays a mean-field transition, whereas the critical exponents extracted from NRG were non-mean-field-like and obeyed hyperscaling. Subsequent NRG calculations for the spin-boson [14] and Ising-symmetric Bose-Fermi Kondo model [7] confirmed this claim. Such a breakdown of quantum-to-classical mapping has consequences not only for quantum-dissipative systems, but also for Kondo lattice

models studied within extended dynamical mean-field theory, where non-mean-field critical behavior is at the heart of so-called local quantum criticality [9].

The purpose of this Letter is twofold: (i) We present a novel and accurate quantum Monte Carlo (QMC) method to study the low-temperature properties of the sub-Ohmic spin-boson model, and (ii) we determine its critical exponents at the QPT using this method together with finite temperature scaling and reconfirm the correctness of the quantum-to-classical mapping for $s < 1/2$.

The spin-boson Hamiltonian is defined as

$$H = \Delta \frac{\hat{\sigma}^x}{2} + \frac{\hat{\sigma}^z}{2} \sum_i \lambda_i (\mathbf{a}_i + \mathbf{a}_i^+) + \sum_i \omega_i \mathbf{a}_i^+ \mathbf{a}_i, \quad (1)$$

where $\sigma^{x,z}$ are Pauli spin-1/2 operators, $\mathbf{a}_i^+$, $\mathbf{a}_i$ are bosonic creation and annihilation operators, Δ the tunnel matrix element, and ω_i the oscillator frequencies of the bosonic degrees of freedom. The spin-bath coupling via the λ_i is determined by the spectral function for the bath:

$$J(\omega) = \pi \sum_i \lambda_i^2 \delta(\omega - \omega_i) = 2\pi\alpha \cdot \omega_c^{1-s} \omega^s \quad (2)$$

for $0 < \omega < \omega_c$ and $J(\omega) = 0$ otherwise. α represents the coupling strength to the dissipative bath and ω_c is a cutoff frequency. The spectral function with $s = 1$ represents an Ohmic bath, and with $s < 1$ a sub-Ohmic bath. A system described by (1) and (2) displays for $s \leq 1$ a QPT at a critical coupling strength $\alpha_c(s, \Delta, \omega_c)$.

Consider a general Hamiltonian of the form

$$H = \Gamma \hat{\sigma}^x + G(\hat{\sigma}^z, \underline{\hat{a}}, \underline{\omega}), \quad (3)$$

where Γ is the transverse field strength, $\Gamma = \Delta/2$ in (1), $\underline{\hat{a}}$ and $\underline{\omega}$ a set of Hermitian operators and parameters, respectively, like the Bose operators and frequencies in the SB model, and G an arbitrary function.

The partition function for this Hamiltonian is derived by implicitly performing the limit of an infinite number of time slices in its Suzuki-Trotter representation [15–17] and yields the imaginary time path integral (PI)

$$Z = \text{Tr}_{\hat{\sigma},\hat{a}} \exp(-\beta H) = \int \mathcal{D}\sigma(\tau) \exp(-S_{\underline{\omega}}[\sigma(\tau)]), \quad (4)$$

where $S_{\underline{\omega}}[\sigma(\tau)]) = -\ln\text{Tr}_{\hat{a}} \exp[\int_0^\beta d\tau G(\sigma(\tau), \hat{a}, \underline{\omega})]$ and $\mathcal{D}\sigma(\tau)$ denotes a Poissonian measure on the space of spin-1/2 world lines, i.e., two-valued functions $\sigma(\tau) \in \{+1, -1\}$ of the imaginary time $\tau \in [0, \beta]$ as sketched in Fig. 1(a) and characterized by $n \geq 0$ spin flips at times $0 < \tau_1, \ldots, \tau_n < \beta$. The intervals $\Delta\tau_i = \tau_{i+1} - \tau_i$ obey a Poissonian statistics $P(\Delta\tau) = \Gamma^{-1} \exp(-\Gamma\Delta\tau)$ with mean value $1/\Gamma$ [16]. The PI (4) can be sampled by generating realizations of such world lines and accepting them according to their "Boltzmann"-weight $\exp(-S_{\underline{\omega}}[\sigma(\tau)])$. More efficient sampling procedures like cluster algorithms are based on this principle [16].

For a general transverse Ising model (without coupling to a dissipative bath) $G(\hat{\sigma}^z)$ represents just the "classical" energy $E(\hat{\sigma}^z)$ that is diagonal in the z-representation of the spin-1/2 degrees of freedom and $S[\sigma(\tau)] = \int_0^\beta d\tau E(\sigma(\tau))$. This form holds for an arbitrary number of spins and for arbitrary spin-spin interactions.

In the case of the SB model (1) and (2), the trace over the oscillator degrees of freedom yields [2] $S_{\underline{\omega}} = S_{SB}$ with

$$S_{SB}[\sigma(\tau)] = -\int_0^\beta d\tau \int_0^\tau d\tau' \sigma(\tau) K_\beta(\tau - \tau') \sigma(\tau'). \quad (5)$$

$K_\beta(\tau)$ imposes long-range interactions in imaginary time:

$$K_\beta(\tau) = \int_0^\infty d\omega \frac{J(\omega)}{\pi} \frac{\cosh(\frac{\hbar\beta}{2}\omega[1 - 2\tau/\beta])}{\sinh(\frac{\hbar\beta}{2}\omega)}. \quad (6)$$

It has the symmetry $K(\beta - \tau) = K(\tau)$ and the asymptotics $K(\tau) \propto \tau^{-(1+s)}$ for $\tau_c \ll \tau \ll \beta$, where $\tau_c = 2\pi/\omega_c$. For $\tau < \tau_c$ the Kernel $K(\tau)$ is regularized via the frequency cutoff ω_c in (2) and approaches a constant for $\tau \to 0$.

An efficient way of sampling the PI (4) is a cluster algorithm based on [16]. It is a generalization of the
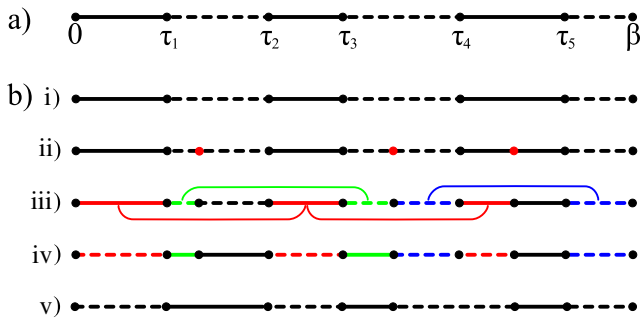

a)

b) i)
   ii)
   iii)
   iv)
   v)

FIG. 1 (color online). (a) Realization of an imaginary time world line of a spin-1/2 in a transverse field. (b) Sketch of the continuous time cluster update: (i) Starting configuration. (ii) Random insertion of new potential spin flips (red dots) with Poissonian statistics. (iii) Connection of segments with probabilities given by Eq. (7). Different colors indicate the resulting clusters. (iv) Each cluster is flipped with probability 1/2 (the blue one was not flipped). (v) Resulting new imaginary time world line.

Swendsen-Wang cluster algorithm [18] to continuous time world lines, which has to incorporate the long-range interactions [19] and in which not individual spins but the world line segments are connected during the cluster-forming procedure. It is sketched in Fig. 1(b): Starting from a world line $\sigma(\tau)$ new potential spin flips are introduced according to a Poissonian statistics, then segment-pairs of equal spin are "connected" with probability

$$p(s_I, s_{II}) = 1 - \exp\left(-2\int_a^b d\tau \int_c^d d\tau' K_\beta(\tau - \tau')\right). \quad (7)$$

where a, b, and c, d denote the limits of segment S_I and S_{II}, respectively. Finally, the connected clusters are identified and flipped with probability $1/2$. All potential spin-flip times that do not represent real spin flips are then removed. We implemented this algorithm and tested it by comparing results with those obtained with conventional Monte Carlo procedures in discrete imaginary time extrapolated to an infinite number of time slices. We analyzed the sampling characteristics of the algorithm for the kernel (6) with (2) over the whole range $0 < s < 1$ and found that world line configurations decorrelate on average after 5 updates as sketched in Fig. 1(b). The data presented below represent averages over 10^5–10^6 updates.

To study the phase transition in the sub-Ohmic spin-boson model ($s < 0.5$) we utilize the finite-β scaling forms for observables close to the critical point $\alpha = \alpha_c$

$$\langle O \rangle_{T,\alpha} = \beta^{x_O} g_O(\beta^{y_t^*}\delta), \quad (8)$$

where $\delta = (\alpha - \alpha_c)/\alpha_c$ denotes the distance from the critical point, x_O and g_O are the scaling exponent and scaling function of the observable O, respectively. The exponent y_t^* is $1/\nu$ below the upper critical dimension ($s > 1/2$), ν being the correlation length exponent, and $y_t^* = 1/\nu + (1/2 - s)$ above it ($s < 1/2$) [19].

We use the dimensionless ratio of moments $Q = \langle m^2 \rangle^2 / \langle m^4 \rangle$, which has $x_Q = 0$ and is therefore asymptotically independent of temperature at $\delta = 0$, to locate the critical point α_c as shown for $s = 0.2$ in Fig. 2(a). This estimate for α_c is then used to perform the finite-β scaling analysis for Q, $Q = \tilde{Q}(\beta^{y_t^*}\delta)$ the magnetization $m = \langle |m| \rangle = \beta^{y_h^*-1}\tilde{m}(\beta^{y_t^*}\delta)$ and the susceptibility $\chi = \beta\langle m^2 \rangle = \beta^{2y_h^*-1}\tilde{\chi}(\beta^{y_t^*}\delta)$, where y_h^* is the magnetic exponent. The data collapse that one obtains with the mean-field values for the exponents y_t^* and y_h^*

$$y_t^* = 1/2, \qquad y_h^* = 3/4 \quad (9)$$

is good, as shown Figs. 2(b)–2(d). At the critical point $\alpha = \alpha_c$ the scaling forms predict $\chi \propto T^{-x}$ with $x = 2y_h^* - 1 = 1/2$, which is clearly confirmed by our data displayed in Fig. 2(d): $\chi T^{1/2}$ collapses onto one point at $\delta = 0$. Moreover the scaling forms imply at $T = 0$: $\chi \propto |\alpha - \alpha_c|^{-\gamma}$ with $\gamma = (2y_h^* - 1)/y_t^* = 1$, which is demonstrated in Figs. 3(a)–3(c) for different values of $s < 1/2$, and $m \propto (\alpha - \alpha_c)^{\beta_m}$ for $\alpha > \alpha_c$ with $\beta_m = -(y_h^* - 1)/y_t^* = 1/2$, which is demonstrated in Fig. 3(d).

Next we allow for an unbiased fit of the critical exponents to our data, including corrections to scaling as in [19]. We determined y_t^* and y_h^* by finite-β scaling of $\partial Q / \partial \alpha (\alpha = \alpha_c) \propto \beta^{y_t^*}$ and $\chi(\alpha = \alpha_c) \propto \beta^{2y_h^* - 1}$. The results confirm (9) within the error bars for the whole range of $s < 1/2$ that we studied. Only close to $s = 1/2$ the finite-β scaling analysis is impeded by the presence of logarithmic corrections at the upper critical dimension. Figures 4(a) and 4(b) show the resulting estimates for the exponents $1/\nu = y_t^* - (1/2 - s)$ and $\beta_m = -(y_h^* - 1)/y_t^*$ in comparison with the NRG predictions of [13].

Although our results for the critical exponents of the sub-Ohmic bath obtained with our continuous imaginary time algorithm deviate from the NRG prediction, results for the phase diagram match: In Fig. 4(c) our estimates for the critical coupling α_c are compared with those obtained with the NRG method [13]; they agree very well.

We confirmed the scenario described here for other values of Δ and ω_c, and also for smooth frequency cutoffs as well as for other kernels (6), like one that has a regularization in time $[K(\tau) = 0$ for $\tau < \tau_c]$ rather than in frequency. We also found that the limit $\omega_c \rightarrow \infty$ (or $\tau_c \rightarrow 0$) exists and is approached smoothly and fast, and conclude that, concerning the critical exponents, the regularization does not play a significant role.

We also implemented a conventional QMC algorithm in discrete time (with a finite number of Trotter time slices M) and found that for any fixed value of $\Delta \tau = \beta / M$ mean-field exponents describe the scaling at the critical point for $s < 1/2$ (see also [19,20]). Moreover we found that the extrapolation $M \rightarrow \infty$ of numerical data for Q, m and χ

obtained for fixed M reproduces perfectly the results obtained with our continuous time algorithm and that the convergence is smooth and fast (with $1/M$, as expected).

Our conclusion therefore is that the quantum-to-classical mapping does not fail in the sub-Ohmic spin-boson model. The question remains, why the NRG calculation presented in [12,13] yields apparently correct results for quantities like the critical coupling, i.e., the phase diagram [see Fig. 4(c)], but fails to predict the correct critical exponents in the case $s < 1/2$.

We believe the problem is rooted in a shortcoming of the present NRG implementation. Because of the truncation of the bosonic Hilbert space, the NRG—while correctly describing the delocalized phase— is unable to capture the physics of localized phase for $s < 1$ [21]. Technically, a finite $\langle \sigma^z \rangle$ implies a mean shift of the bath oscillators which diverges in the low-energy limit. Hence, the NRG results are expected to be reliable as far as they do not involve properties of the localized fixed point.

The analysis of critical exponents in Ref. [13] now assumed that all exponents are properties of the critical fixed point, and that the fixed-point spectrum at criticality is captured by NRG. However, the first assumption is *invalid* for the order-parameter related exponents β_m and δ_m *if* the critical fixed point is Gaussian (like in a ϕ^4 theory above its upper critical dimension). Then, the order-parameter amplitude is controlled by a dangerously irrele-
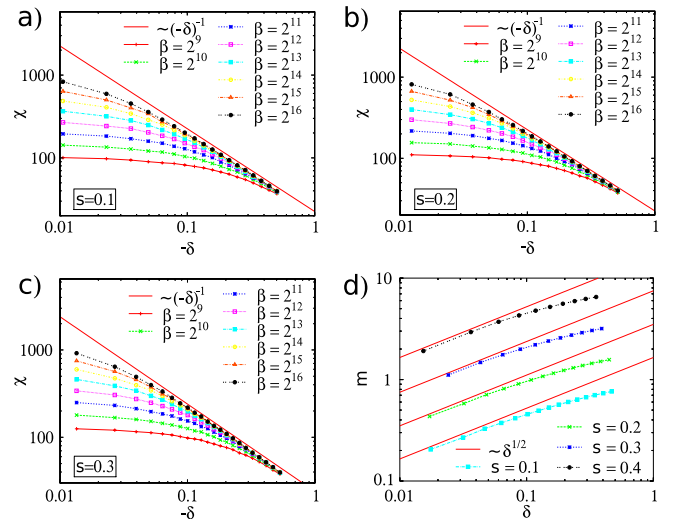
FIG. 3 (color online).   (a)–(c) Data for the susceptibility χ as a function of the distance from the critical point $\delta > 0$ (i.e., in the delocalized phase) for $s = 0.1$ (a), $s = 0.2$ (b) and $s = 0.3$ for different values of β (Δ and ω_c as in Fig. 2). For increasing inverse temperature β the data points approach the straight line, which is the zero temperature behavior $\chi \propto \delta^{-1}$. (d) Magnetization m as a function of $\delta > 0$ (i.e., in the localized phase) for $\beta = 2^{16}$ for different values of s (multiplied with 2, 4 and 8 for $s = 0.2$, $s = 0.3$ and $s = 0.4$, respectively, for better visibility). The straight lines are guides for the eye proportional to the zero temperature behavior $(\alpha - \alpha_c)^{-1/2}$. Shown are only the data that are free from finite-β corrections.
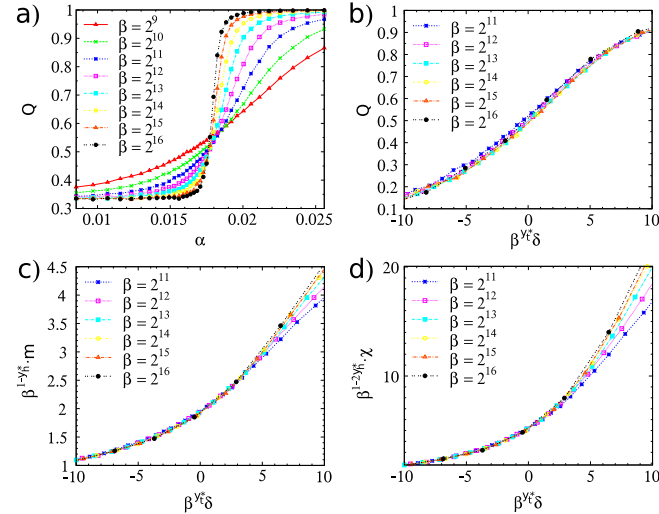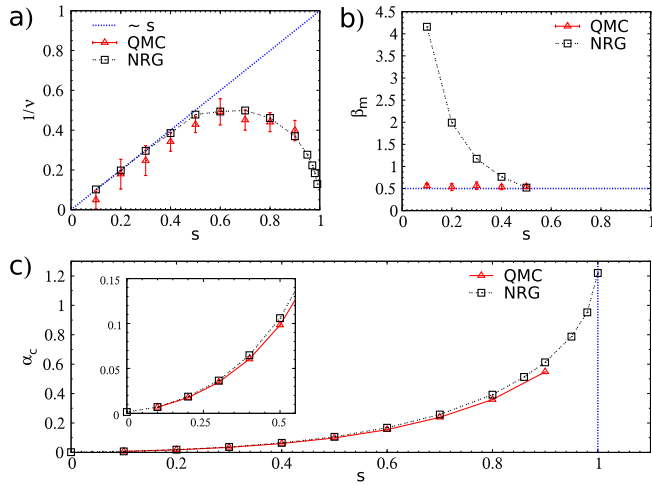

FIG. 2 (color online).   Results for the spin-boson model for $s = 0.2$ and $\Delta = 0.1$. (a) Moment-ratio Q as a function of the coupling constant α for different values of β. The critical coupling is at $\alpha_c = 0.0175 \pm 0.0002$. (b)–(c) Finite β-scaling for the moment-ratio Q, magnetization m and susceptibility χ according to (8). The values for the critical exponents are $y_t^* = 0.5$, $y_h^* = 0.75$. For large positive values of the scaling variable corrections to scaling are stronger.

FIG. 4 (color online). (a)–(b) Numerical estimates of the critical exponents $1/\nu$ and β_m as a function of s. Triangles: QMC result (from finite temperature scaling of the QMC data as described in the text); squares: RG results (from [13], cf. also [7]); straight lines: mean-field values for $s < 1/2$. (c) Critical coupling strength α_c as a function of s for the SB model (1) and (2) with $\omega_c = 1$ and $\Delta = 0.1$. Triangles: QMC result; squares: NRG results for fixed NRG discretization parameter $\Lambda = 2$ (from [12]). Performing the limit $\Lambda \rightarrow 1$ moves the NRG estimates for α_c slightly downward.

vant variable, and β_m and δ_m are properties of the flow towards the localized fixed point, which in turn is not correctly captured by NRG. The second assumption is correct for the NRG ground state [21], but fails for excited states which are used to calculate the exponent x. Therefore, the values of β_m, δ_m, and x extracted from (present) NRG calculations are unreliable.

Considering that the NRG calculations nevertheless gave well-defined power laws which were moreover consistent with hyperscaling, it is worth asking for the underlying reason. We conjecture that the artificial Hilbert-space truncation, which limits $\langle \sigma^z \rangle$, is equivalent to an operator which is exactly marginal at criticality in the ϕ^4 language. Near criticality, this has no consequences below the upper critical dimension, $s > 1/2$, as the quartic interaction is relevant here, but for $s < 1/2$ the marginal operator instead dominates over the quartic term. It is easy to show that an exactly marginal coupling leads to $y_h^* = (1 + s)/2 - y_i$ with $y_i = 0$ such that hyperscaling is fulfilled, while y_t^* takes its mean-field value—this is what characterizes the set of NRG critical exponents [13]. (The correct result $y_h^* = 3/4$ for $s < 1/2$ implies $y_i = (2s - 1)/4$ arising from the dangerously irrelevant variable.) The above reasoning is supported by analyzing fermionic impurity models, which naturally have the property that a Hilbert-space constraint limits the field response. For instance, a resonant-level model with power-law bath density of states, which is controlled by a stable intermediate-coupling fixed point, shows hyperscaling for all bath exponents [22]. Finally, the analytical RG argument in Ref. [13], based on an epsilon-expansion for small s,

predicted non-mean-field exponents obeying hyperscaling for a related reason: While the RG equations (9)–(11) of Ref. [13] are correct, the subsequent analysis overlooked the presence of the dangerously irrelevant variable, resulting again in the incorrect $y_h^* = (1 + s)/2$.

To conclude, we have, using an efficient and accurate continuous time cluster Monte Carlo algorithm, shown that the quantum-to-classical mapping *is* valid for the sub-Ohmic spin-boson model. The presence of a dangerously irrelevant variable for $s < 1/2$ impedes the correct extraction of the critical exponents with current versions of the NRG method—work on its extension to reliably treat the localized phase is in progress.

[1] A. J. Leggett *et al.*, Rev. Mod. Phys. **59**, 1 (1987).
[2] U. Weiss, *Quantum Dissipative Systems* (World Scientific, Singapore, 1999).
[3] K. Le Hur, Phys. Rev. Lett. **92**, 196804 (2004); M. R. Li, K. Le Hur, and W. Hofstetter, Phys. Rev. Lett. **95**, 086406 (2005).
[4] M. Thorwart and P. Hänggi, Phys. Rev. A **65**, 012309 (2001); T. A. Costi and R. H. McKenzie, Phys. Rev. A **68**, 034301 (2003).
[5] S. Tornow, N. H. Tong, and R. Bulla, Europhys. Lett. **73**, 913 (2006).
[6] For a review see: R. Bulla, T. A. Costi, and T. Pruschke, Rev. Mod. Phys. **80**, 395 (2008).
[7] M. T. Glossop and K. Ingersent, Phys. Rev. Lett. **95**, 067202 (2005); Phys. Rev. B **75**, 104410 (2007).
[8] M. T. Glossop and K. Ingersent, Phys. Rev. Lett. **99**, 227203 (2007).
[9] Q. Si *et al.*, Nature (London) **413**, 804 (2001); Phys. Rev. B **68**, 115103 (2003).
[10] L. Zhu *et al.*, Phys. Rev. Lett. **93**, 267201 (2004); J.-X. Zhu *et al.*, Phys. Rev. Lett. **99**, 227204 (2007); S. Kirchner and Q. Si, Phys. Rev. Lett. **100**, 026403 (2008).
[11] M. Suzuki, Prog. Theor. Phys. **56**, 1454 (1976).
[12] R. Bulla, N. H. Tong, and M. Vojta, Phys. Rev. Lett. **91**, 170601 (2003).
[13] M. Vojta, N. H. Tong, and R. Bulla, Phys. Rev. Lett. **94**, 070604 (2005).
[14] K. Le Hur, P. Doucet-Beaupre, and W. Hofstetter, Phys. Rev. Lett. **99**, 126801 (2007).
[15] C. Pich *et al.*, Phys. Rev. Lett. **81**, 5916 (1998).
[16] H. Rieger and N. Kawashima, Eur. Phys. J. B **9**, 233 (1999).
[17] F. Krzakala *et al.*, Phys. Rev. B **78**, 134428 (2008).
[18] R. H. Swendsen and J.-S. Wang, Phys. Rev. Lett. **58**, 86 (1987).
[19] E. Luijten and H. W. J. Blöte, Phys. Rev. B **56**, 8945 (1997).
[20] P. Werner and M. Troyer (private communication); S. Kirchner and Q. Si, arXiv:0808.2647.
[21] R. Bulla *et al.*, Phys. Rev. B **71**, 045122 (2005).
[22] L. Fritz and M. Vojta, Phys. Rev. B **70**, 214427 (2004).